

Inverse transition in the two dimensional dipolar frustrated ferromagnet

Sergio A. Cannas,^{1,*} Marianella Carubelli,^{1,†} Orlando V. Billoni,^{1,‡} and Daniel A. Stariolo^{2,§}

¹*Facultad de Matemática, Astronomía y Física, Universidad Nacional de Córdoba,
Instituto de Física Enrique Gaviola (IFEG-CONICET)
Ciudad Universitaria, 5000 Córdoba, Argentina*

²*Departamento de Física, Universidade Federal do Rio Grande do Sul
and National Institute of Science and Technology for Complex Systems
CP 15051, 91501-970 Porto Alegre, RS, Brazil[¶]*

(Dated: November 14, 2018)

We show that the mean field phase diagram of the dipolar frustrated ferromagnet in an external field presents an inverse transition in the field-temperature plane. The presence of this type of transition has recently been observed experimentally in ultrathin films of Fe/Cu(001). We study a coarse-grained model Hamiltonian in two dimensions. The model supports stripe and bubble equilibrium phases, as well as the paramagnetic phase. At variance with common expectations, already in a single mode approximation, the model shows a sequence of paramagnetic-bubbles-stripes-paramagnetic phase transitions upon lowering the temperature at fixed external field. Going beyond the single mode approximation leads to the shrinking of the bubbles phase, which is restricted to a small region near the zero field critical temperature. Monte Carlo simulations results with a Heisenberg model are consistent with the mean field results.

PACS numbers: 75.70.Ak, 75.30.Kz, 75.70.Kw

Keywords: ultrathin magnetic films, inverse transition, mean field, stripes and bubbles

I. INTRODUCTION

It is well known that dipolar forces in ferromagnetic systems favor the appearance of domain structures¹. In particular, in thin ferromagnetic films with uniaxial out of plane anisotropy two kind of patterns are usually observed, stripes and bubbles²⁻⁴. Stripes are the stable structures at low temperatures in absence of external fields^{5,6}. When an external magnetic field is present, a bubble phase may appear in the field-temperature phase diagram⁷. Regarding the $h - T$ mean field phase diagram, Garel and Doniach⁷ using a single mode approximation obtained that, as the external field is increased, a sequence of stripes-bubbles-paramagnet phases have successively the lower free energy below the critical temperature. Furthermore, the transition lines stripes-bubbles and bubbles-paramagnet decay monotonically with growing temperature, until both meet at a critical point T_c at $h = 0$. This behavior was partially confirmed by simulations of a dipolar lattice gas^{8,9} and more recently in the dipolar Ising model¹⁰. Interestingly, this seemingly established picture of the mean field phase diagram was recently put in question, both from experimental results on ultrathin films of Fe/Cu(001)^{4,11} and also from a theoretical point of view¹². The experiments on Fe/Cu(001) show convincingly an inverse transition sequence paramagnet-modulated-paramagnet when cycling in temperature at fixed external applied field. In a recent work, Portmann *et al.*¹² addressed the question about the origin of this inverse symmetry breaking transition in the context of a scaling hypothesis proposed by the authors. The critical field line $h_c(T)$, which separates the modulated from the paramagnetic phases is a consequence of the balance between the dipolar energy,

which favors the presence of domains, and the external field energy, which favors a uniform state. Within the proposed scaling form for the energies, this immediately implies that $h_c \propto M(T)/\lambda(T)$, where $M(T)$ and $\lambda(T)$ are the saturation magnetization inside a domain and the modulation length at zero field respectively. As the temperature grows, the magnetization is first nearly constant while the modulation length strongly diminishes, but on approaching the critical temperature M decreases faster than λ . Then the critical field line $h_c(T)$ first grows, passes through a maximum, and finally decays to zero at T_c . This means that the phase diagram has a dome-like shape, instead of the monotonic behavior predicted by Garel and Doniach work⁷. This behavior was anticipated by Abanov *et al.*⁶ and, in a different context, by Andelmann *et al.*¹³, but no further analysis of their origin or implications was done.

Motivated by these new results, we have reconsidered the mean field phase diagram of a coarse-grained Hamiltonian for the dipolar frustrated ferromagnet. We have gone beyond the usual single mode approximation, by considering the effects of higher harmonics in the modulation profiles. This is expected to be crucial in the context of the recently proposed scaling hypothesis. The single mode approximation is valid very near the critical point. In particular, in this approximation, the modulation length is independent of temperature, at variance with the experimental observed behavior. Furthermore, in this condition the scaling hypothesis is not expected to be applicable and a dome-shape of the phase diagram is not to be expected. Actually, *even in the single mode approximation*, the mean field critical field line passes through a maximum and an inverse transition is obtained, as was shown by Andelman *et al.*¹³ (even when

they studied a different system, both problems are equivalent, as shown in the supplementary material), and verified by ourselves. Going beyond the single mode approximation we determined the variation of the modulation length with temperature, and show that a few modes are enough in order to get an asymptotic behavior. Our results are in agreement with previous ones^{14,15}. The most notable effect of including higher harmonics is the shrinking of the bubbles phase in the $h - T$ plane. The triple point, already present in the single mode approximation, shifts to higher temperature, and the whole region where the bubble phase is the thermodynamically stable one is considerably reduced near the critical temperature. The overall results seem to indicate a lose of stability of the bubbles phase at low temperatures. These results are compared with Monte Carlo simulations of a Heisenberg model with exchange and dipolar interactions. A tentative phase diagram is presented, which is in qualitative agreement with some of the mean field predictions. In particular, it was not possible to find bubbles at low tem-

peratures for the parameters values studied. At higher temperatures bubbles seem to be the stable phase for not too low fields.

The plan of the paper is as follows: in Section II we introduce the mean field model. In IIA we compute the profiles of the modulated solutions and the variation of the stripe width with temperature by considering higher harmonics in the variational solution at zero external field. In IIB we present the results for the $h - T$ phase diagram. In Section III we show results of Monte Carlo simulations of a Heisenberg model and compare them with the mean field calculations. In Section IV we present our conclusions.

II. MEAN FIELD PHASE DIAGRAM

The mean field model is defined by the Landau-Ginzburg free energy:

$$F[\phi] = \frac{1}{2} \int d^2\mathbf{x} \left\{ (\nabla\phi(\mathbf{x}))^2 + r_0\phi^2(\mathbf{x}) + \frac{u}{2}\phi^4(\mathbf{x}) \right\} + \frac{1}{2\delta} \int d^2\mathbf{x} \int d^2\mathbf{x}' \phi(\mathbf{x})\phi(\mathbf{x}')J'(|\mathbf{x} - \mathbf{x}'|) - \int d^2\mathbf{x} h(\mathbf{x})\phi(\mathbf{x}) \quad (1)$$

where the scalar field $\phi(\mathbf{x})$ represents, *e.g.*, the out-of-plane magnetization density in a magnetic thin film with perpendicular anisotropy. The terms between brackets model ferromagnetic behavior in the continuum limit, where $r_0 \propto T - T_F$, T_F being the Curie temperature. $J'(|\mathbf{x} - \mathbf{x}'|)$ is a (translational invariant) competing interaction, which introduces frustration and is responsible

for modulated patterns at low temperatures. It may represent, *e.g.*, the dipolar interaction in an ultrathin film $J'(r) \propto 1/r^3$. δ is the ratio between the ordering (*e.g.*, exchange) and the competing (*e.g.*, dipolar) interaction intensities and $h(\mathbf{x})$ is an external field. In the Fourier representation the Landau-Ginzburg free energy reads:

$$F[\phi] = \frac{1}{2} \sum_{\mathbf{k}} A(k)\phi(\mathbf{k})\phi(-\mathbf{k}) + \frac{u}{4L^2} \sum_{\mathbf{k}_1} \sum_{\mathbf{k}_2} \sum_{\mathbf{k}_3} \phi(\mathbf{k}_1)\phi(\mathbf{k}_2)\phi(\mathbf{k}_3)\phi(-\mathbf{k}_1 - \mathbf{k}_2 - \mathbf{k}_3) - \sum_{\mathbf{k}} h(\mathbf{k})\phi(-\mathbf{k}) \quad (2)$$

where

$$\phi(\mathbf{x}) = \frac{1}{L} \sum_{\mathbf{k}} \phi(\mathbf{k}) e^{i\mathbf{k}\cdot\mathbf{x}} \quad (3)$$

$$A(k) = r_0 + k^2 + \frac{J(k)}{\delta} \quad (4)$$

and

$$J(k) = \int d^2\mathbf{r} J'(r) e^{-i\mathbf{k}\cdot\mathbf{r}} \quad (5)$$

The equilibrium configuration is given by the set of amplitudes $\{\phi(\mathbf{k})\}$ that minimize the free energy (2). We will assume that $J(k)$ is such that $A(k)$ has a single minimum at $k = k_m$. At high enough temperatures and in the absence of an external field, the uniform configuration (paramagnetic) $\phi(\mathbf{k}) = 0$ is the absolute minimum. The critical temperature at which the uniform solution becomes unstable is given by the condition $A(k_m) = 0$. Hence, without loss of generality we can assume the general form

$$A(k) = -b\tau + c(k - k_m)^2 \quad (6)$$

where $\tau \equiv (T_c - T)/T_c$ and $b, c > 0$. This form should be valid close enough of T_c . We will consider a uniform external field h , so that $h(\mathbf{k}) = L h \delta_{\mathbf{k},0}$. For large enough values of h , a uniform solution $\phi(\mathbf{k}) = 2 L m_0 \delta_{\mathbf{k},0}$, with

$$2A(0) m_0 + 8 u m_0^3 = h, \quad (7)$$

is expected to be the absolute minimum. For low values of h and below the critical temperature $\tau > 0$ one expects a modulated solution with a characteristic wave vector $k = k_0$ to become the absolute minimum, where $k_0 \rightarrow k_m$ when $\tau \rightarrow 0$. We will consider two different types of variational solutions: a striped configuration

$$\phi_s(\mathbf{x}) = 2 \sum_{n=0}^{\infty} m_n \cos(n \mathbf{k}_0 \cdot \mathbf{x}), \quad (8)$$

and a bubble type configuration

$$\phi_b(\mathbf{x}) = 2 \sum_{n=0}^{\infty} m_n \sum_{i=1}^3 \cos(n \mathbf{q}_i \cdot \mathbf{x}), \quad (9)$$

where \mathbf{q}_i are three vectors satisfying $|\mathbf{q}_i| = k_0$ and $\sum_{i=1}^3 \mathbf{q}_i = 0$. The Fourier transforms of both configurations are given by

$$\phi_s(\mathbf{k}) = L \sum_{n=0}^{\infty} m_n [\delta_{\mathbf{k}, n \mathbf{k}_0} + \delta_{\mathbf{k}, -n \mathbf{k}_0}] \quad (10)$$

$$\phi_b(\mathbf{k}) = L \sum_{n=0}^{\infty} m_n \sum_{i=1}^3 [\delta_{\mathbf{k}, n \mathbf{q}_i} + \delta_{\mathbf{k}, -n \mathbf{q}_i}] \quad (11)$$

Replacing Eqs.(10) and (11) into Eq.(2), we get the mean field free energy in terms of the infinite set of amplitudes $\{m_n\}$ and k_0 , which can be considered as variational parameters. Then, truncating Eqs.(10) and (11) to some maximum order n_{max} (i.e., imposing $m_n = 0 \forall n > n_{max}$) we obtain variational expressions at different levels of approximation for the stripes and bubbles free energies respectively. The complete expressions and some examples are presented in the supplementary material. Assuming that those are the only possible equilibrium states, we can calculate the equilibrium phase diagram by minimizing and comparing the free energies for each type of solution to the same level of approximation n_{max} . Except for a few particular analytical approximations, in most of the cases free energy minimization was done numerically using a generalized simulated annealing optimization procedure¹⁶. All the numerical results shown in this section were done for $b = 1$, $u = 1$ and $c/k_m = 0.1$, which appropriately represents the spectrum of a two dimensional Ising model with exchange and dipolar interactions¹⁷. Some checks performed with different values of the parameters did not show qualitative differences.

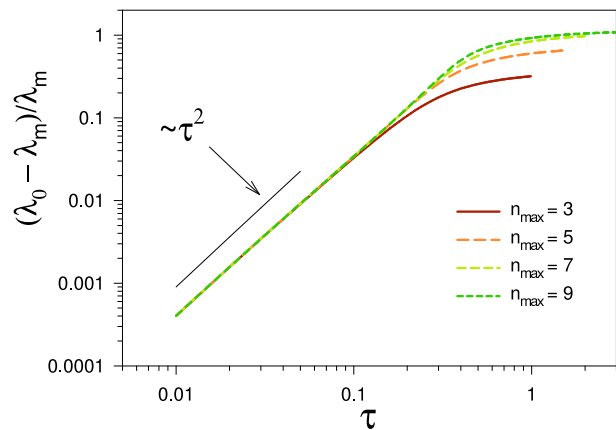


FIG. 1: (Color online) Stripe width variation with temperature at zero field for different values of n_{max} .

A. Zero field solutions: stripe width variation

In order to check the limits of validity of the present variational method we first analyze the limit of zero magnetic field. In this case the free energy of the bubbles solution is always larger than the striped one. Also, due to the up-down symmetry of the system, all the harmonics in Eq.(10) with n even do not contribute: $m_{n \text{ even}} = 0$.

Direct minimization of Eq.(2) respect to the fields $\phi(\mathbf{k})$ leads to

$$A(k)\phi(\mathbf{k}) = -\frac{u}{L^2} \sum_{\mathbf{k}_1} \sum_{\mathbf{k}_2} \phi(\mathbf{k}_1)\phi(\mathbf{k}_2)\phi(\mathbf{k} - \mathbf{k}_1 - \mathbf{k}_2) \quad (12)$$

Replacing Eqs.(12) into Eq.(2) we obtain

$$F = \frac{1}{4} \sum_{\mathbf{k}} A(k) |\phi_0(\mathbf{k})|^2 \quad (13)$$

where $\phi_0(\mathbf{k})$ are the solutions of Eqs.(12). When $T > T_c$ we have $A(k) > 0 \forall k$ and therefore, from Eq.(13), the minimum free energy corresponds to the paramagnetic solution $\phi_0(\mathbf{k}) = 0 \forall k$. When $T = T_c$, $A(k_m) = 0$ and a single mode solution with wave vector $k_0 = k_m = \pi/\lambda_m$ becomes the minimum of the free energy. As the temperature is further decreased new modes will contribute to the minimum free energy solution and the stripe width $\lambda_0 \equiv \pi/k_0$ is expected to increase. We performed a numerical optimization considering up to five modes, i.e., up to $n_{max} = 9$. The resulting stripe width $\lambda_0 - \lambda_m$ as a function of temperature is shown in Fig.1. The results become almost independent of n_{max} for $n_{max} > 9$.

For temperatures close enough of to T_c we see that $\lambda_0 - \lambda_m \sim \tau^2$, in qualitative agreement with the Bragg-Williams approximation of the dipolar frustrated Ising model^{14,15} and also with experimental results on Fe on Cu(100) ultrathin magnetic films¹⁴. However, at variance with the dipolar frustrated Ising model, where a

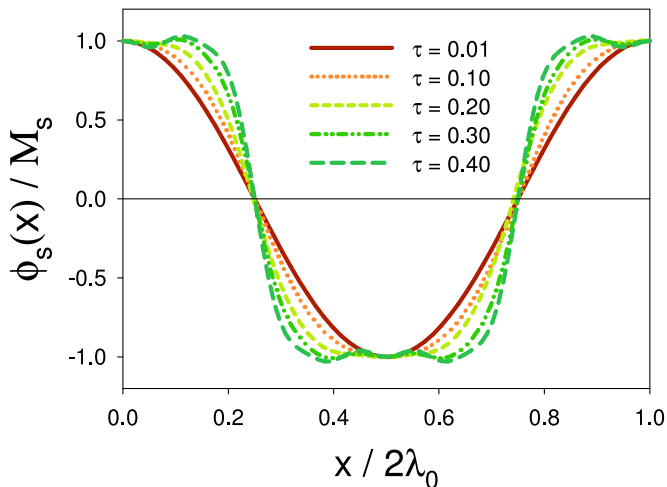


FIG. 2: (Color online) Change in the magnetization profile with temperature at zero field for $n_{max} = 9$.

crossover to a faster increasing regime (probably exponential) is expected as the temperature decreases, in the present model the stripe width crosses over to a saturation regime. Hence, we can take the crossover value of the reduced temperature $\tau \approx 0.4$ as the limit of validity of the present approximation, in the sense of reproducing the behavior close to T_c of a more accurate microscopic model.

In Fig.2 we show the change in the normalized magnetization profile $\phi_s(\mathbf{x})/M_s(T)$, where the saturation magnetization inside a domain is defined as

$$M_s(T) = \phi(\mathbf{x} = 0) = 2 \sum_{n=1}^{n_{max}} m_n. \quad (14)$$

We see how the profile changes from a sinusoidal shape close to T_c towards a sharp wall type (i.e., square wave form) as the temperature decreases. The same qualitative behavior is observed both in the Bragg-Williams solution of the dipolar frustrated Ising model and experimentally¹⁵.

B. Non zero field solutions: phase diagram

The minimum level of approximation in this case is to consider only one mode, i.e., only m_0 and m_1 in Eqs.(10) and (11) are taken different from zero. It is straightforward to verify that minimization conditions in this case imply $k_0 = k_m$ for any value of the temperature. In other words, at this level of approximation no stripe width variation with temperature is observed. The phase diagram under this approximation was first obtained by Garel and Doniach⁷ and later by Andelman *et al.*¹³ (see supplementary material). We reproduce such phase diagram in the inset of Fig.3 for later comparison with an

improved phase diagram. All the transition lines are first order. The most remarkable fact is the absence of a bubbles phase (B) for low enough temperatures, namely at low temperatures there is a single transition line from the stripes (S) to the uniform (U) phase that joins in a triple point with the S-B and B-U transition lines located close to T_c . Our single mode phase diagram differs from the originally obtained in Ref. 7 (and widely accepted in the literature) but agrees with that from Ref. 13. Interestingly, as mentioned in the Introduction, already at a single mode approximation an inverse transition is obtained, in qualitative agreement with recent experiments. Also note that the triple point, at which the bubbles phase cease to minimize the mean field free energy, corresponds to $T/T_c \sim 0.75$ ($\tau \sim 0.25$), well inside the limit of validity of the continuum model as discussed in the previous section. Of course, the single mode approximation is probably not reliable at this temperature.

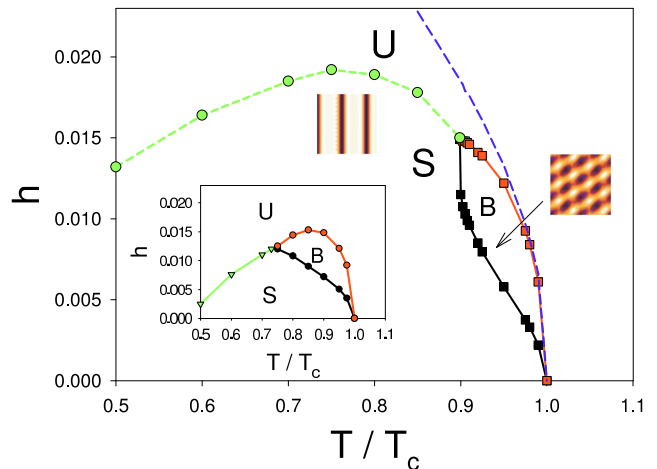


FIG. 3: (Color online) Phase diagram in the three modes $n_{max} = 3$ approximation. Some typical configurations at the stripes and bubble phases are shown. The blue dashed line correspond to the S spinodal line. The upper B spinodal line lies slightly below the S spinodal line, but both lines are indistinguishable at the present scales. The inset shows the phase diagram in the one mode $n_{max} = 1$ approximation.

To improve such phase diagram we considered a three modes approximation $n_{max} = 3$, namely, we numerically minimized the stripes and bubbles solutions (10) and (11) with respect to the set of parameters $\{k_0, m_0, m_1, m_2, m_3\}$. Those minimal free energies were compared between them and against the uniform solution (U) from Eq.(5). As in the zero field case, the width of the stripes solution exhibit a quadratic variation with temperature for any value of h . We also verified that the inclusion of further modes in the solutions decreases the free energy for all values of T and h . The resulting phase diagram is shown in Fig.3. The main differences with the one mode phase diagram are the shift of the maximum from the B-U to the S-U transition lines and the shrinking of the B region with the corresponding movement of

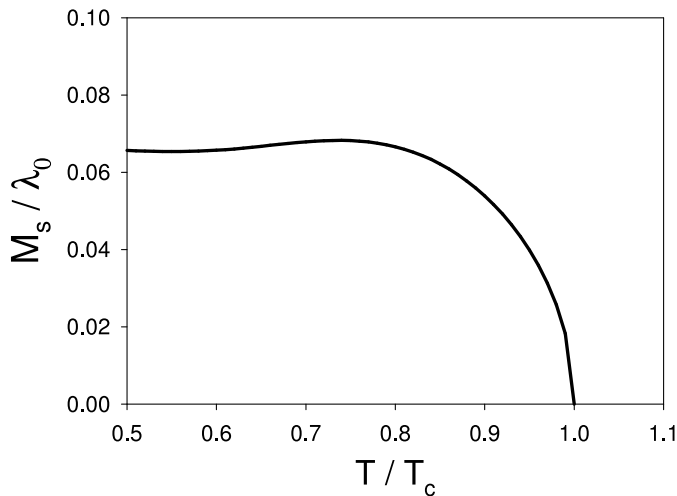


FIG. 4: Ratio M_s/λ_0 at zero field as a function of temperature for $n_{max} = 9$.

the triple point towards the critical temperature. Notice that the location of both the maximum in the S-U line ($\tau \sim 0.25$) and the triple point ($\tau \sim 0.1$) falls inside the estimated temperature range of validity of the model. We also observed a strong metastability of both the S and B phases in all the analyzed temperature range

$$\mathcal{H} = -\delta \sum_{\langle i,j \rangle} \vec{S}_i \cdot \vec{S}_j + \sum_{(i,j)} \left[\frac{\vec{S}_i \cdot \vec{S}_j}{r_{ij}^3} - 3 \frac{(\vec{S}_i \cdot \vec{r}_{ij})(\vec{S}_j \cdot \vec{r}_{ij})}{r_{ij}^5} \right] - \eta \sum_i (S_i^z)^2 \quad (15)$$

where the exchange and anisotropy constants are normalized relative to the dipolar coupling constant, $\langle i,j \rangle$ stands for a sum over nearest neighbors pairs of sites in a square lattice with $N = L \times L$ sites, (i,j) stands for a sum over *all distinct* pairs and $r_{ij} \equiv |\vec{r}_i - \vec{r}_j|$ is the distance between spins i and j . All the simulations were done using the Metropolis algorithm and periodic boundary conditions were imposed on the lattice by means of the Ewald sums technique. For intermediate values of the anisotropy η this model exhibits an in plane - out of plane reorientation transition¹⁸ at zero magnetic field. In the large η limit and for low temperatures, the local magnetization inside the domains is mainly in the out of plane direction, and therefore the behavior is expected to be comparable to the scalar Landau-Ginzburg model of the previous section. We choose $\delta = 3$ and $\eta = 8$. For this set of parameters the system is far away from the reorientation transition, and there is a direct phase transition from the striped state to a perpendicular disordered state at $T_c = 1.13$ ¹⁸. The simulations were carried

at high values of h . The spinodal line for the S phase is shown in Fig.3. The upper spinodal line for the B phase lies slightly below the previous one (both lines are indistinguishable on the scales of the figure). Both the U and B phases are metastable for $T < T_c$ at any value of $h > 0$ below the transition lines.

Finally, to check the scaling hypothesis proposed in Ref. 12 we calculated the ratio M_s/λ_0 at zero field as a function of temperature, from the results of the previous section. Consistently with the scaling hypothesis, we see from Fig.4 that this ratio exhibit a maximum around $T/T_c \sim 0.75$, like the S-U transition line in the phase diagram from Fig.3. As we lower the temperature the ratio increases again because the modulation length saturates while M_s monotonously increases, in an unphysical way.

III. MONTE CARLO SIMULATIONS IN A DIPOLAR HEISENBERG MODEL

In order to compare the mean field results with the behavior of a specific microscopic model we performed Monte Carlo (MC) simulations using a Heisenberg model with exchange and dipolar interactions, as well as uniaxial out of plane anisotropy. The model, which describes an ultrathin magnetic film (see Ref.18 and references therein) can be characterized by the dimensionless Hamiltonian:

out for $L = 40$. To characterize the magnetic states we calculate the out-of-plane magnetization:

$$M_z \equiv \frac{1}{N} \sum_{\vec{r}} \langle S^z(\vec{r}) \rangle, \quad (16)$$

and the orientational order parameter¹⁸:

$$O_{hv} \equiv \left\langle \left| \frac{n_h - n_v}{n_h + n_v} \right| \right\rangle \quad (17)$$

where $\langle \dots \rangle$ stands for a thermal average, n_h (n_v) is the number of horizontal (vertical) pairs of nearest neighbor spins with antialigned perpendicular component, *i.e.*,

$$n_h = \frac{1}{2} \sum_{\vec{r}} \{1 - \text{sig}[S^z(r_x, r_y), S^z(r_x + 1, r_y)]\} \quad (18)$$

and a similar definition for n_v , where $\text{sig}(x, y)$ is the sign of the product of x and y .

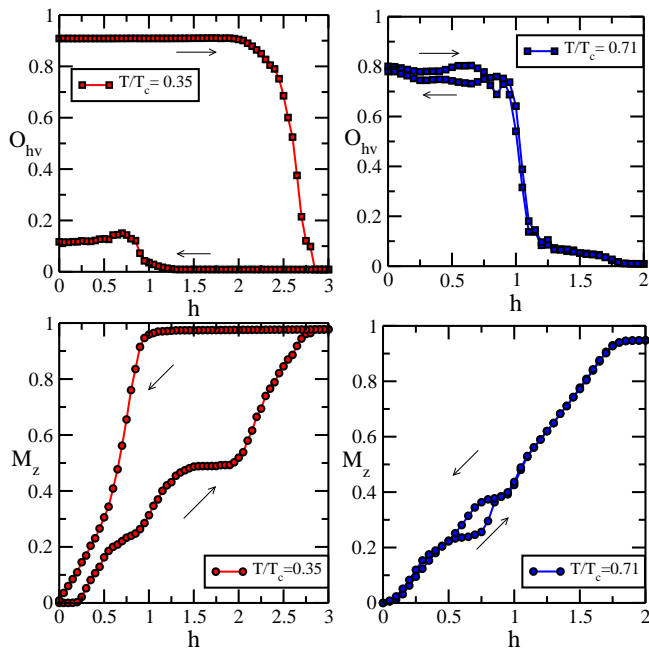


FIG. 5: (Color online) Cycles of orientational order parameter O_{hv} (upper panels) and perpendicular magnetization M_z (lower panels) as a function of field h , for two temperatures: $T/T_c = 0.35$ (left panels) and $T/T_c = 0.71$ (right panels). The arrows indicate the sense of field variation in the cycle.

We performed field cycles at fixed temperatures according to the following protocol. The system is initialized at a stripes configuration (the ground state at $h = 0$). The field is increased from zero to a h_{max} and then decreased back to zero, using a ladder procedure with a step variation $\Delta h = 0.05$. At each fixed field the system is thermalized during $t_e = 5 \times 10^5$ Monte Carlo Step (MCS) and then we calculate averages over the next $t_m = 10^4$ MCS. We also performed similar temperature cycles at fixed field. Using these cycles together with a visual inspection of the corresponding spin configuration we obtained the $h - T$ phase diagram.

In Fig. 5 we show the typical (field cycling) behavior of O_{hv} and M_z for temperatures close to and far away from T_c , namely $T/T_c = 0.35$ and $T/T_c = 0.71$. The cycles for $T/T_c = 0.35$ show a strong hysteretic behavior, while the curves for $T/T_c = 0.71$ show only a weak hysteresis on a small range of h .

In the low temperature regime ($T/T_c = 0.35$) we see that O_{hv} drops to zero at the same field value for which M_z saturates into $M_z = 1$, signaling the transition into an uniform state. As the field increases we see the presence of small plateaus in the magnetization followed by sudden jumps. These jumps correspond to an increase in the width of stripes with spins aligned to the field preserving the orientational order, as evidenced in the behavior of O_{hv} . Such increase in the size of domains aligned with the external field is in agreement with experimental observations¹¹. In this temperature regime

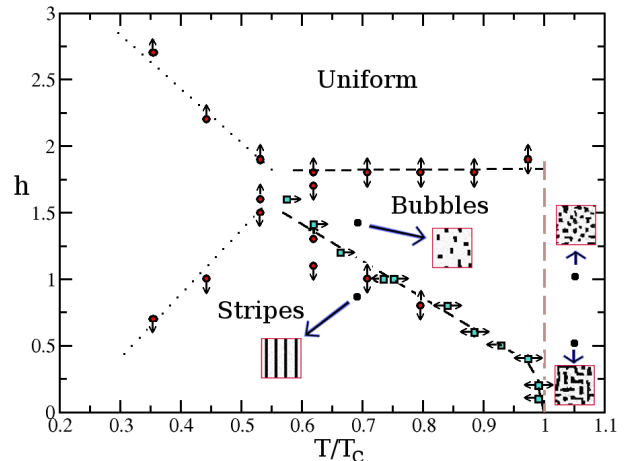


FIG. 6: (Color online) MC phase diagram h vs temperature for the dipolar Heisenberg model with $\delta = 3$ and $\eta = 8$. Different symbols correspond to different calculation methods of order parameter O_{hv} and perpendicular magnetization M_z : circle for variation in field h at constant temperature and squares for variation in temperature at constant field. The arrows indicate the directions of parameter variations. We show some typical spin configuration at different phases. The vertical dashed line is schematic and shows the cross over between regions where bubbles and disordered states can be well differentiated. The dotted lines correspond to the loss of stability (probably spinodal lines) of the stripes (upper line) and uniform (lower line) states when the field is increased (decreased).

no bubbles states are observed and the system goes from a stripes order to a uniform state, with a strong metastability in both the uniform and the stripes states.

When $T/T_c = 0.71$ we observe a clear transition from a striped state to a state without orientational order at a well defined value of the field $h \sim 1$, without saturation in the magnetization. A visual inspection of the configurations shows indeed that, between the stripes order at low field and the uniform state at high field, the system displays bubble domains in the range $1 \lesssim h \lesssim 1.75$. Using this criterion we calculate the field values for the stripes-bubbles and bubbles-uniform transitions for each temperature.

In Fig.6 we show the phase diagram calculated with the above described procedure. The absence of hysteresis in the temperature range $0.5 < T/T_c < 1$ (except very close to T_c) allows us to determine with a rather good precision the stripes-bubbles and the bubbles-uniform phase boundaries. Very close to T_c it is very difficult to distinguish between the bubbles state and a uniform state with fluctuations, due to finite size effects. For temperatures above T_c (but close to it) and zero field, the disordered state presents a tetragonal liquid structure^{18,19}. As the

field increases the size of the domains antialigned with the field shrinks, until they break into a disordered arrange (liquid like) of antialigned domains in a ferromagnetic background aligned with the field. Close enough to T_c such state is indistinguishable from a regular arrange of bubbles for small system sizes, both by visual inspection or quantitative (e.g., structure factor) calculations. A detailed study with larger systems sizes is under way and will be published elsewhere. A similar effect has been observed by MC simulations in the dipolar frustrated Ising model¹⁰. The dashed line in Fig.6 is schematic and shows the crossover region.

On the other hand, at low temperatures ($T/T_c < 0.5$) we did not find any evidence of bubbles states. Although we cannot exclude the possibility of bubbles states hidden by the strong metastability of both the stripes and uniform states, our results appear to be consistent with the existence of a single stripes-uniform first order phase transition at low temperatures, as predicted by the mean field calculation of the previous section.

IV. CONCLUSIONS

In view of recent theoretical and, specially, experimental results, the mean field phase diagram of a two dimensional system with competing interactions in an external field was reconsidered. Although known from nearly 30 years ago⁷, we have found important differences from the behavior usually accepted. Interestingly, our results are in qualitative agreement with experimental results and point once more to the relevance of the mean field behavior in this kind of systems.

First of all, we have found that, already in the single mode approximation, the external field- temperature phase diagram shows an inverse symmetry breaking transition between paramagnetic and modulated phases, as recently predicted based on scaling arguments and confirmed by experiments on ultrathin ferromagnetic films^{4,11,12}. The presence, and experimental relevance, of the inverse transitions, was not considered previously in the context of the mean field phase diagram. From a theoretical point of view, although the generic presence of inverse transitions in this kind of systems was proposed as a consequence of scaling in the behavior of the characteristic lengths with temperature¹², we have found that the $h-T$ phase diagram shows a maximum even when scaling is not expected to occur. This seems to be a very basic

property of systems with competing interactions in external fields. However, it is worth to stress that, when more accurate solutions (that correctly describe the modulation length variation with temperature) are considered, the scaling hypothesis correctly predicts the location of the maximum in the symmetry breaking transition line between paramagnetic and modulated phases.

Second, we have confirmed that the modulation length strongly depends on temperature below the paramagnetic-modulated transition, even in the presence of external fields. The quadratic dependence of the modulation length with temperature is obtained with and without external field. This dependence is already obtained considering a few harmonics which change the profile of the order parameter from a simple cosenoidal shape near T_c to a square-like shape as the temperature decreases. At low temperatures domain walls become sharp and our continuum approximation breaks down.

Third, going beyond the single mode approximation, we have shown that the overall phase diagram does not change the main characteristics, but the stability lines of the different phases do change. In particular, the region where the bubbles phase is the thermodynamically stable one shrinks to a small region near T_c when three modes are considered in the variational solution.

Doing Monte Carlo simulations of an Heisenberg model with perpendicular anisotropy we have found overall qualitative agreement between simulations and mean field results. In particular, field cycles at low temperatures show strong hysteretic behavior between stripes and paramagnetic phases, showing no sign of bubbles. Although such strong metastability makes it very difficult to determine whether the transition line presents a maximum or not, its existence cannot be excluded from the present results. At higher temperatures hysteresis is greatly suppressed and the saturation is reached from the low- h stripes phase passing through a bubbles phase at intermediate fields. While it is difficult to guarantee equilibrium in the system studied, the behavior observed is in general agreement with mean field predictions of the thermodynamic phases. Large scale simulations would be very valuable to confirm our preliminary results and the overall picture from the mean field calculation.

This work was partially supported by grants from FONCYT/ANPCYT (Argentina), CONICET (Argentina), SeCyT, Universidad Nacional de Córdoba (Argentina) and CNPq (Brazil).

* Electronic address: cannas@famaf.unc.edu.ar

† Electronic address: marianela.carubelli@gmail.com

‡ Electronic address: billoni@famaf.unc.edu.ar

§ Electronic address: daniel.stariolo@ufrgs.br

¶ Research Associate of the Abdus Salam International Centre for Theoretical Physics, Trieste, Italy

¹ A. Hubert and R. Schafer, *Magnetic Domains* (Springer-

Verlag, Berlin, 1998).

² O. Portmann, A. Vaterlaus, and D. Pescia, *Nature* **422**, 701 (2003).

³ J. Choi, J. Wu, C. Won, Y. Z. Wu, A. Scholl, A. Doran, T. Owens, and Z. Q. Qiu, *Phys. Rev. Lett.* **98**, 207205 (2007).

⁴ N. Saratz, A. Lichtenberger, O. Portmann, U. Ramsperger,

- A. Vindigni, and D. Pescia, Phys. Rev. Lett. **104**, 077203 (2010).
- ⁵ Y. Yafet and E. M. Gyorgy, Phys. Rev. B **38**, 9145 (1988).
- ⁶ A. Abanov, V. Kalatsky, V. L. Pokrovsky, and W. M. Saslow, Phys. Rev. B **51**, 1023 (1995).
- ⁷ T. Garel and S. Doniach, Phys. Rev. B **26**, 325 (1982).
- ⁸ M. M. Hurley and S. J. Singer, Phys. Rev. B **46**, 5783 (1992).
- ⁹ A. D. Stoycheva and S. J. Singer, Phys. Rev. E **65**, 036706 (2002).
- ¹⁰ R. Díaz-Méndez and R. Mulet, Phys. Rev. B **81**, 184420 (2010).
- ¹¹ N. Saratz, U. Ramsperger, A. Vindigni, and D. Pescia, Phys. Rev. B **82**, 184416 (2010).
- ¹² O. Portmann, A. Gölzer, N. Saratz, O. V. Billoni, D. Pescia, and A. Vindigni, Phys. Rev. B **82**, 184409 (2010).
- ¹³ D. Andelman, F. Brochard, and J. F. Joanny, J. Chem. Phys. **86**, 3673 (1987).
- ¹⁴ O. Portmann, A. Vaterlaus, and D. Pescia, Phys. Rev. Lett. **96**, 047212 (2006).
- ¹⁵ A. Vindigni, N. Saratz, O. Portmann, D. Pescia, and P. Politi, Phys. Rev. B **77**, 092414 (2008).
- ¹⁶ C. Tsallis and D. A. Stariolo, Physica A **233**, 395 (1996).
- ¹⁷ S. A. Cannas, D. A. Stariolo, and F. A. Tamarit, Phys. Rev. B **69**, 092409 (2004).
- ¹⁸ M. Carubelli, O. V. Billoni, S. A. Pighín, S. A. Cannas, D. A. Stariolo, and F. A. Tamarit, Phys. Rev. B **77**, 134417 (2008).
- ¹⁹ S. A. Cannas, M. F. Michelon, D. A. Stariolo, and F. A. Tamarit, Phys. Rev. B **73**, 184425 (2006).